

**J4.11**

**Analyzing Surface Wind Fields Near Lower Cook Inlet And Kodiak Waters Using SAR**

Eddie Zingone

Weather Forecast Office, National Weather Service, Anchorage Alaska

Gary L. Hufford

Alaska Region Headquarters, National Weather Service, Anchorage Alaska

**ABSTRACT**

The unique combination of terrain and dynamic weather systems makes the coastal waters of lower Cook Inlet and Kodiak Island a complex and difficult place to forecast coastal winds. In addition, there are only a few real-time in situ observations available. However, this region has a large concentration of maritime operations that require accurate, high resolution wind information. Spaceborne synthetic aperture radar (SAR) - based surface wind speed fields, at 200 m resolution, provides detailed location and character of the

wind patterns, regardless of time of day or cloud conditions. Some case studies are presented to demonstrate the usefulness of the SAR-based winds to: 1) greatly improve operational marine forecasts issued for an area where synoptic and mesoscale meteorological events coexist; 2) provide detailed validation of the forecasted coastal winds; and 3) give insight on complex wind patterns and extreme winds that occur in a data sparse area.

*Corresponding author address:* Eddie Zingone, NWS Anchorage WFO, 6930 Sand Lake Road, Anchorage, Alaska 99502-1845. E-mail: Eddie.Zingone@noaa.gov

## 1. Introduction

The unique combination of terrain and dynamic weather systems make the coastal waters of lower Cook Inlet and Kodiak Island a complex and difficult place to forecast. Lower Cook Inlet is a tidal embayment that projects north-northeast for over 240 km into the southcentral coast. The lower Inlet narrows from a maximum width near its mouth of about 140 km to 50 km near Kalgin Island. The Inlet lies between the Chugach and Kenai Mountains to the southeast, the Talkeetna Mountains on the northeast, and the Alaska-Aleutian Range on the northwest. Lower Cook Inlet opens to the southeast into the Gulf of Alaska through Stevenson and Kennedy Entrances flanking the Barren Islands. Lower Cook Inlet is also connected to the southwest with Shelikof Strait, which extends another 270 km to a juncture with the North Pacific Ocean. Shelikof Strait lies between the Aleutian Range to the northwest and Kodiak Island to the southeast. The rough terrain encircling Cook Inlet and Shelikof Strait interacts with the large-scale winds and pressure gradients to produce highly variable regimes on scales of a few kilometers.

There are localized and intense barrier jets, gap winds, and outflow winds (Macklin et al. 1990; Bond and Macklin 1993). Extreme wind speeds can occur over a relatively small area, especially strong northwest gap winds through the Kamishak Gap, a low-lying area through the Aleutian Range connecting southwest Alaska mainland with lower Cook Inlet. The gap winds over the region occur when there is

a low pressure system in the northeastern Gulf of Alaska and a high pressure system in the vicinity of the northern Bering Sea (Fett, 1993). The gap winds are exacerbated when strong northwest cold air advection shoots through the gaps, a common phenomenon from autumn to spring. Northeast winds produce strong outflow in the lower Cook Inlet and Shelikof Strait. There is also an easterly barrier jet along the southern Kenai Peninsula that enters lower Cook Inlet and upper Shelikof Strait.

Very few real-time in situ observations exist in the area. There are three coastal – marine automated network (C-MAN) stations; Augustine Island (AUGA2), Flat Island (FILA2), and Amatuli Island (AMAA2). In addition, there are four reporting coastal towns; Kodiak (PADQ), Seldovia (PASO), Homer (PAHO), and Homer Spit (HBHA2). (See Figure 1 for the station locations). Many wind events are often missed or incorrectly analyzed for this region that has a large concentration of maritime activities that requires accurate, high resolution wind information. Spaceborne synthetic aperture radar (SAR) is well suited for observing coastal sea surface winds in lower Cook Inlet and Kodiak Island waters, regardless of the time of day or cloud conditions.

SAR is an active sensor that transmits microwave radiation in pulses and records the radiation backscattered in the direction of the sensor. A number of papers have been written describing both the positive aspects and deficiencies of SAR (Monaldo 2000; Monaldo et al. 2001). The major obstacle to the SAR

derived wind speeds is the requirement for a prior knowledge of the wind direction. A common operational technique is to determine wind direction using numerical weather prediction (NWP) model derived wind direction. It is well recognized that NWP data can contain significant errors, especially in the vicinity of complex coastlines where the model has difficulty in fully resolving the terrain and its impact on the mesoscale flow (Mass et al. 2002). However, when an analysis is conducted on a small scale and in a limited area, the risks of making directional errors are somewhat reduced.

This paper examines how useful SAR-based winds can be to the operational marine forecast community. Some case studies are conducted to demonstrate utility of the data in the very complex coastal waters of lower Cook Inlet and Kodiak Island where reasonably accurate wind patterns, speeds and speed patterns would otherwise be precluded.

## **2. Methodology**

High resolution wind speed estimates are based on ScanSAR Wide data (100 m resolution) from the SAR sensor onboard the Canadian Space Agency's RADARSAT-1. This SAR is C-band (5.6 cm) and right-looking, with horizontal-horizontal polarization. The SAR data is collected at the SAR facility at the University of Alaska Fairbanks. The SAR-based wind speed image is produced and archived at the John Hopkins University Applied Physics Laboratory's Ocean Remote Sensing Group in near real-time as part of the Alaska SAR Demonstration Project (Pichel

and Clemente-Colon 2000). Methodology used for generating the SAR-based wind speeds as well as the wind speed products can be found at:

[//fermi.jhuapl.edu/sar/stormwatch/web\\_wind/](http://fermi.jhuapl.edu/sar/stormwatch/web_wind/).

Wind direction on the wind speed images uses the wind direction field from the United States Navy's NOGAPS model (Rosmond 1992) and is displayed as an arrow at the latitude/longitude intersection points.

## **3. Case Studies**

We present some case studies for two synoptic scale wind directions (northwest and northeast) over lower Cook Inlet and Kodiak Island to illustrate the utility of the SAR-based wind speeds to: 1) improve coastal marine forecasts; 2) provide validation of the wind forecasts, and 3) further forecaster understanding of local conditions.

### ***a. Northwest Wind Events***

Extreme wind speeds can occur over relatively small areas in southern Cook Inlet (Macklin et al. 1990) during strong northwest winds, especially through the Kamishak Gap, a low-lying area through the Alaska Range. Gap winds also occur throughout much of Shelikof Strait. Case studies 1 and 2 show the utility of SAR-based winds to detect and observe variability in the gap winds.

#### ***i. Northwest Wind Case 1***

Figure 2 shows a SAR-based image of strong northwest winds (> 20m/s) at 1700 UTC, December 12, 1999 coming from Kamishak Gap and diminishing southeastward

as they pass over the Barren Islands. Also note the behavior of the winds in Shelikof Strait. There are strong northwest winds (core speeds >20 m/s) out of a number of gaps in both the northern and southern parts of the Strait that reach across the width of the Shelikof Strait. Much weaker winds are observed in the middle of the Strait due to blockage by 8 volcanoes collectively known as the Katmai Volcano cluster located on the Alaska Peninsula. These volcanoes form a 30 km-long line of contiguous mountains, with elevations ranging from 1830 to 2320 m. Wind shadows along the southern coast of Kodiak Island are also evident in the wind speed image.

Comparing the location of local surface observations in Figure 1 with the gap wind pattern in Figure 2 shows the challenges faced by the forecaster in attempting to analyze the surface wind field in this data sparse region. C-Man FILA2 on Flat Island is in the gap flow but outside of the gap core so that the wind speed is at least 5 m/s less than in the core. AMAA2 on Amatuli Island (part of the Barren Islands) is in the wind shadow of the Island. There are no surface observation sites in Shelikof Strait.

The corresponding synoptic meteorological analysis for 1800 UTC, 12 December, 1999 from the National Centers for Environmental Prediction (NCEP) surface analysis indicated a 63 mb difference in pressure between a 1052 mb high in eastern Russia and a 989 mb low in the northeastern Gulf of Alaska (Fig. 3). Also note the presence of a 1002 mb low southeast of Kodiak Island. This low served to

reduce the pressure gradient across the western Gulf of Alaska and therefore reduce the winds as they passed on the Gulf of Alaska side of Kodiak Island. Without this low, the Kamishak Gap winds would normally extend further in the Gulf (which we will see in the next case study).

## ii. Northwest Wind Case 2

Two major storms (0006 UTC, October 13, 1999 and 0006 UTC, December 24, 1999, respectively) produced gale force winds (>18 m/s) in lower Cook Inlet and Kodiak Island coastal waters with the Kamishak Gap wind (>25 m/s) extending more than 360 km into the Gulf of Alaska as seen in the SAR wind speed fields (Figs. 4 and 5). Gap winds (>17 m/s) in the northern and southern part of Shelikof Strait extended across Kodiak Island well into the Gulf of Alaska. Note the difference in the extent of wind shadowing southeast of Kodiak Island between the two different storms. Winds in the shadow areas were generally less than 6 m/s.

Corresponding NCEP surface analyses at 0006 UTC on both days show the location of both lows in the northeastern Gulf of Alaska to be quite similar (Figs. 6 and 7). There is an absence of a low in the western Gulf that was present in case 1 above. There is a considerable difference in pressure gradient as well as in the northwest position of the high pressure systems. In spite of these differences, the two SAR-based wind speed patterns look remarkably similar (Figs. 4 and 5).

It is evident from the cases studies that when synoptic northwest winds occur over the lower Cook Inlet and Kodiak region, gap winds dominate the mesoscale flow patterns. The few surface observation sites in the area are not well located to detect these mesoscale gaps winds and the wind directions are not resolved by NOGAPS. The SAR-based wind speed patterns are the only source of detailed information on the intensity and extent of the gap winds in the area.

### ***b. Northeast Wind Events***

#### **i. Northeast Wind Case 1**

On October 16, 1999, SAR-based wind speeds from a satellite pass at 0004 UTC show strong northeast winds accelerating down lower Cook Inlet and Shelikof Strait (Fig. 8). The maximum wind speeds (~ 36 m/s) do not occur in the place of greatest constriction in either lower Cook Inlet or Shelikof Strait, but near their exit regions. Note the 75 km wide strong northeast winds along the southern coast of the Kenai Peninsula that continued southwest past Kodiak Island. There is a distinct speed boundary on the southern edge of these winds where the winds diminish immediately south of the boundary.

The corresponding surface synoptic analysis at 0006 UTC from NCEP is provided in Figure 9. Unlike the northwest wind scenarios, the low pressure system is located in the western Gulf of Alaska very close to Kodiak Island. The high pressure system is found northwest in a similar position to the highs observed in the northwest wind scenarios. The analysis also shows a surface

cold front associated with the low in the western Gulf of Alaska. The location of the cold front in the analysis corresponds to the speed boundary observed in the southeast sector of the SAR-based wind field. The wind speeds decrease immediately behind the cold front (Fig. 8).

#### **ii. Northeast Wind Case 2**

Figure 10 indicates northeast winds accelerating down lower Cook Inlet in the SAR-based wind speed image of 0006 UTC, 1 March 2004. Speeds vary from around 5 m/s near the upper portions of lower Cook Inlet to well over 20 m/s near Augustine Island. A wind shadow is clearly evident southwest of Augustine Island. The presence of the wind shadow removes any doubt that the winds are from the northeast in this area. Directly adjacent to the Kenai Peninsula coastline is a sharply defined narrow band of markedly larger wind speed (>20 m/s). This band appears to be a mesoscale jet. There is also a very distinct speed boundary on the seaward edge of the speed band. This speed band appears to converge with the northeast winds flowing down Cook Inlet in the wind speed image and wind speed at the convergence is 15 m/sec. The wind speed image reveals two small gap flows of 15 m/s extending northwest across the Kenai Peninsula into Kachemak Bay

A corresponding NCEP surface analysis is not provided in this paper for this 1 March 2004 case. However, the SAR derived wind imagery for this date provides an excellent look at the complex wind field where many

features can be easily discerned even without the surface analysis map to compliment it.

#### **4. Results and Discussion**

Case studies over the lower Cook Inlet and Kodiak Island waters for two synoptic flow regimes, northwest and northeast winds, were examined to demonstrate the utility of SAR-based wind speeds in discerning coastal mesoscale speed patterns and extremes, with special interest in gap winds, barrier jets, and outflow winds in complex terrain. Such information is invaluable to mariners that ply these waters whose activities are significantly affected by high wind speeds.

The synoptic pattern described in the northwest wind case 1 on 12 December, 1999, is important for the operational forecaster to recognize. The development of the secondary low south of Kodiak Island often occurs when cold air advects across the Alaska Peninsula into the Gulf of Alaska and upper level atmospheric support is present. This pressure pattern reduces the extent of the mesoscale Kamishak Gap winds offshore, something an operational forecaster would have a difficult time recognizing without the aid of SAR-based winds. When the pressure pattern does not have a secondary low in the western Gulf and strong cold air advection shoots through the gaps (a common phenomenon from autumn to spring) the gap winds can extend great distances offshore into the Gulf of Alaska. In the northwest wind case 2, both October 13 and December 24 1999 storms were associated with Kamishak Gap winds that extended more than 360 km offshore. These

SAR-based wind speed patterns agree well with past studies that inferred the location of the Kamishak Gap winds from visible and microwave satellite imagery (Fett, 1993). The results from northwest wind case 2 underscore the point that when a moderate to strong low is located in the northeastern Gulf of Alaska and high pressure is located northwest in the vicinity of the Bering Sea, strong northwesterly winds will develop through the Kamishak Gap and extend well offshore. Gap winds will also occur in the northern and southern portions of Shelikof Strait. SAR-based wind speed patterns are the only source of detailed information on the intensity and extent of the gap winds in the area virtually from the coast to offshore.

During a synoptic northeast wind pattern over lower Cook Inlet and Shelikof Strait strong outflow occurs in both waters. A barrier jet occurs adjacent to the Kenai Peninsula and continues into lower Cook Inlet and upper Shelikof Strait. This barrier jet can be very narrow (<10 km) like during the 1 March, 2004 case, or extend over 70 km in the October 16, 1999 case. The wind direction inferred in the SAR-wind speed patterns, suggest that the likely wind direction within the barrier jet is cyclonic, paralleling the shore. The very distinct speed boundary on the seaward edge of the barrier jet is probably due to onshore synoptic flow meeting the mesoscale coastline parallel flow within the barrier jet. The interaction of these winds not only produces the seaward speed boundary, but also results in two small gap flows of 15 m/s extending northwest across the Kenai Peninsula and into

Kachemak Bay (Fig.10). SAR-based winds are the only tool the operational forecaster in Alaska has to provide a detailed look at high resolution wind speed that can detect features of only a few km next to the coast.

## **5. Summary**

This paper demonstrates the utility of high resolution (100 m) SAR-based wind speeds to: aid the operational forecaster in making more accurate coastal marine forecasts; provide validation of forecasted coastal winds; and give insight on local complex wind patterns and extreme winds that would normally not be detected in a data sparse area. In addition, the SAR- based wind patterns often provided the

wind direction of features such as gap winds, barrier jets, and outflows in relation to the complex terrain. This information is extremely important to mariners who ply the waters of lower Cook Inlet and Kodiak Island and must be prepared to make rapid adjustments to their activities that can be influenced by strong winds: i.e. tugs towing barges and fishing vessels trawling nets.

Access to SAR winds for this project is due to the Alaska SAR Demonstration Project. The Demonstration Project at this time is dependent on foreign satellite data. The results from this study strongly support the need for a domestic satellite equipped with SAR for operational use.

## References

- Bond, N.A., and S.A. Macklin, 1993: Aircraft observations of offshore-directed flow near Wide Bay, Alaska. *Mon. Wea. Rev.*, **121**, 150-161.
- Fett, R., 1993: The Kamishak Gap winds as depicted in DMSP OLS and SSM/I data. *Int. Jour. Rem. Sens.*, **14**, 403-423.
- Macklin, S.A., N.A. Bond, and J.P. Walker, 1990: Structure of a low-level jet over lower Cook Inlet, Alaska. *Mon. Wea. Rev.*, **118**, 2568-2578.
- Mass, C.F., D. Ovens, K. Westrick, and B.A. Colle, 2002: Does increasing horizontal resolution produce more skillful forecasts? *Bull. Amer. Meteor. Soc.*, **83**, 407-430.
- Monaldo, F.M., 2000: The Alaska SAR demonstration and near real-time synthetic aperture Winds. The John Hopkins University Technical Digest, **21**, 75-79.
- Monaldo, F.M., D.R. Thompson, R.C. Beal, W.G. Pichel, and P. Clemente-Colon, 2001: Comparison of SAR-derived wind speed with model predictions and ocean buoy Measurements. *IEEE Trans. Geosci. Rem. Sens.* **39**, 2587-2600.
- Pichel, W. and P. Clemente-Colon, 2000: NOAA CoastWatch SAR applications and Demonstration. John Hopkins University Technical Digest, **21**, 49-57.
- Rosmond, T.E., 1992: The design and testing of the Navy Operational Global Atmospheric Prediction System. *Wea. Forecasting.*, **7**, 262-272.



Figure Captions.

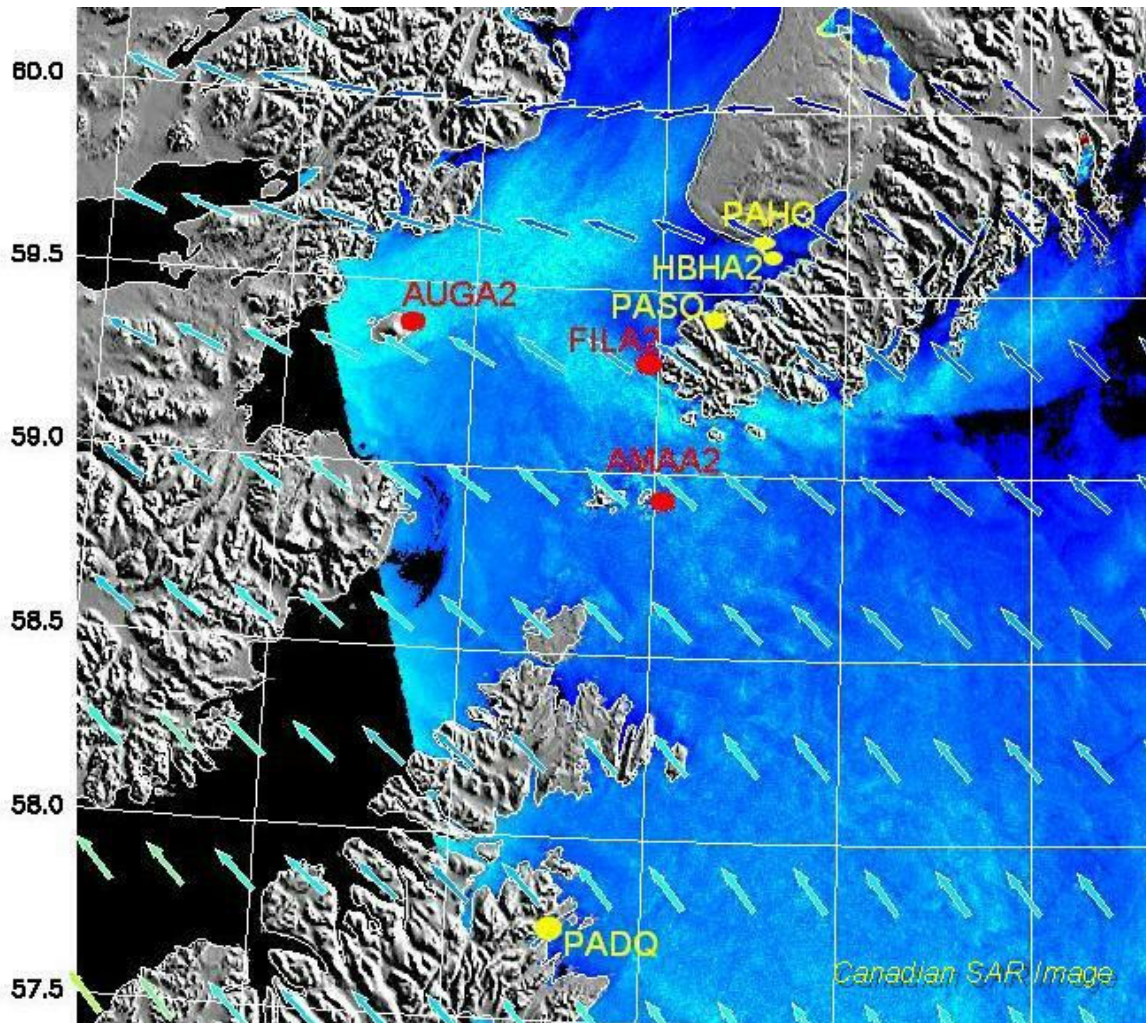


Figure.1

Location of surface observation stations in lower Cook Inlet and Kodiak Island overlain on a SAR-derived wind speed field.

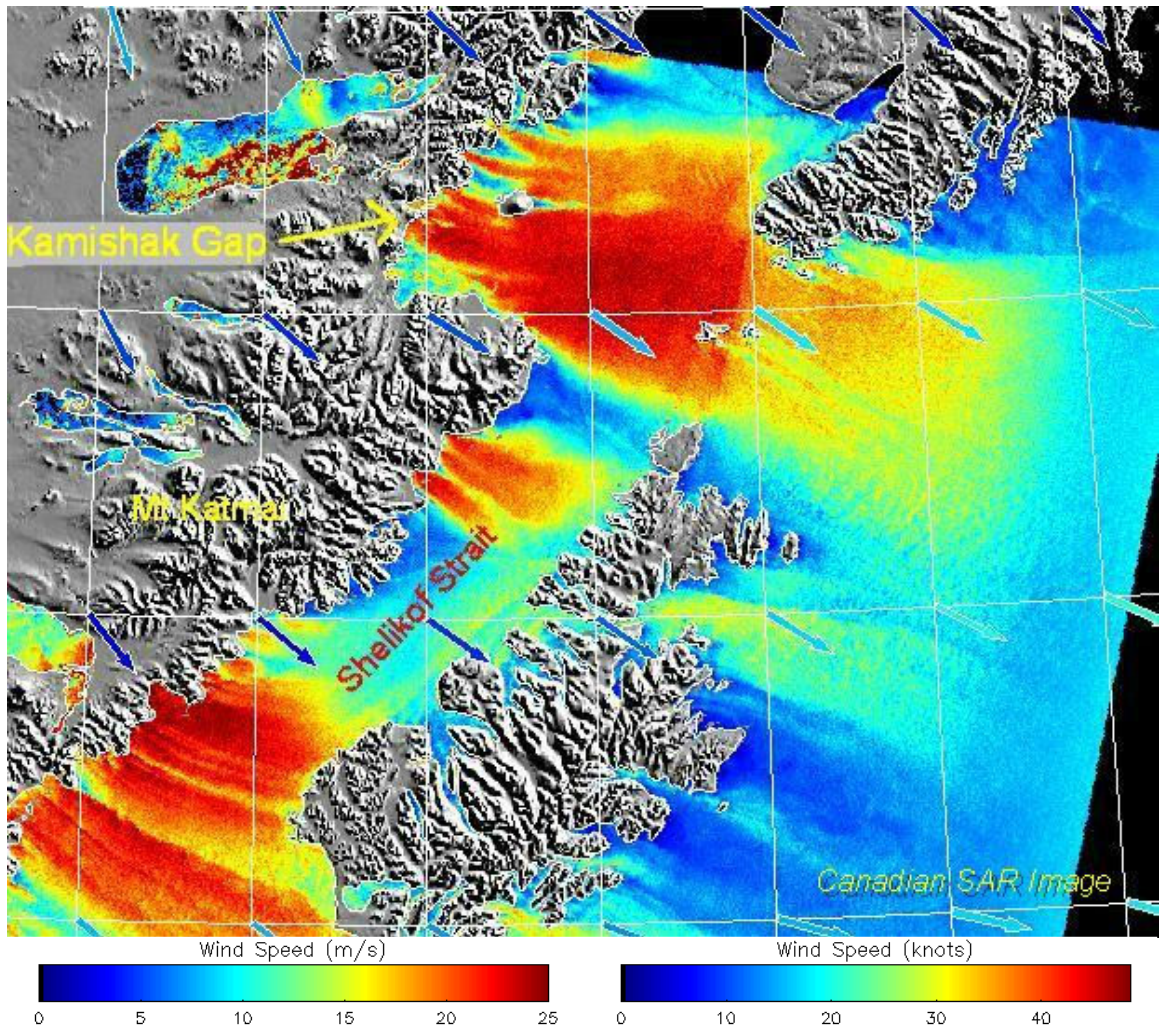


Figure 2.

A strong synoptic northwest wind event at 1700 UTC, 12 December, 1999. A wind speed scale in both m/s and kts is provided on the bottom of the figure.

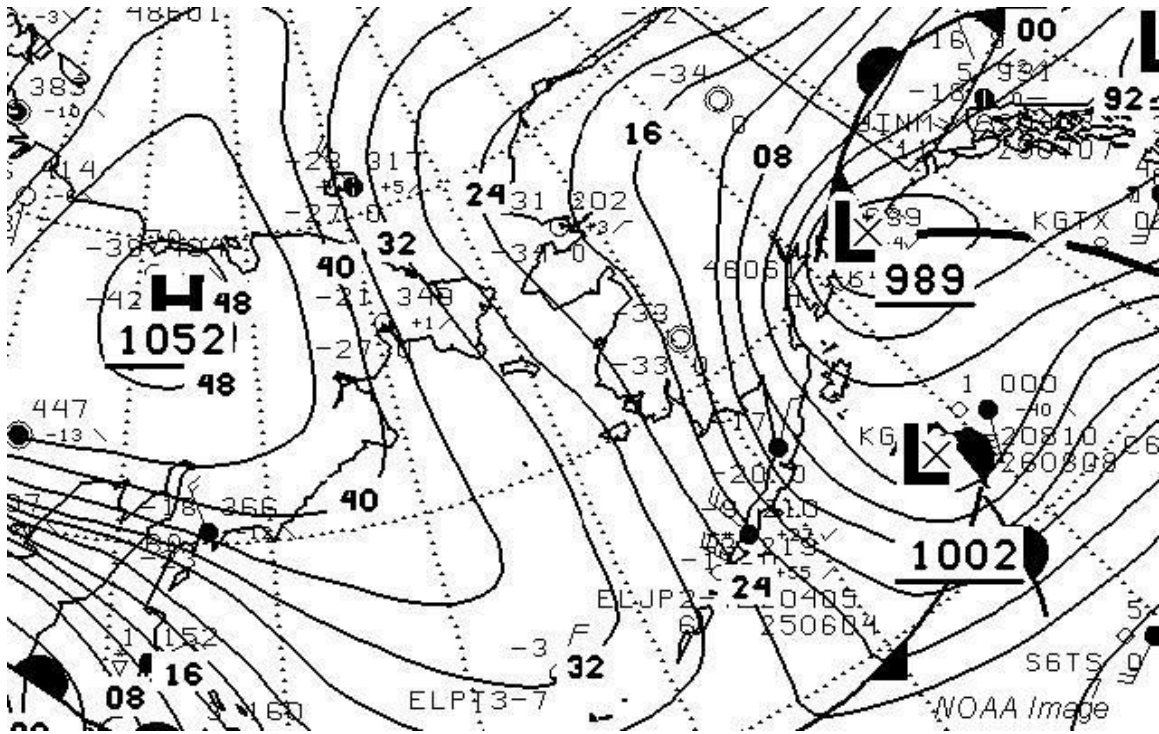


Figure 3.

Corresponding National Centers for Environmental Prediction (NCEP) surface pressure analysis at 1800 UTC, 12 December, 1999 with wind event displayed in Figure 2.

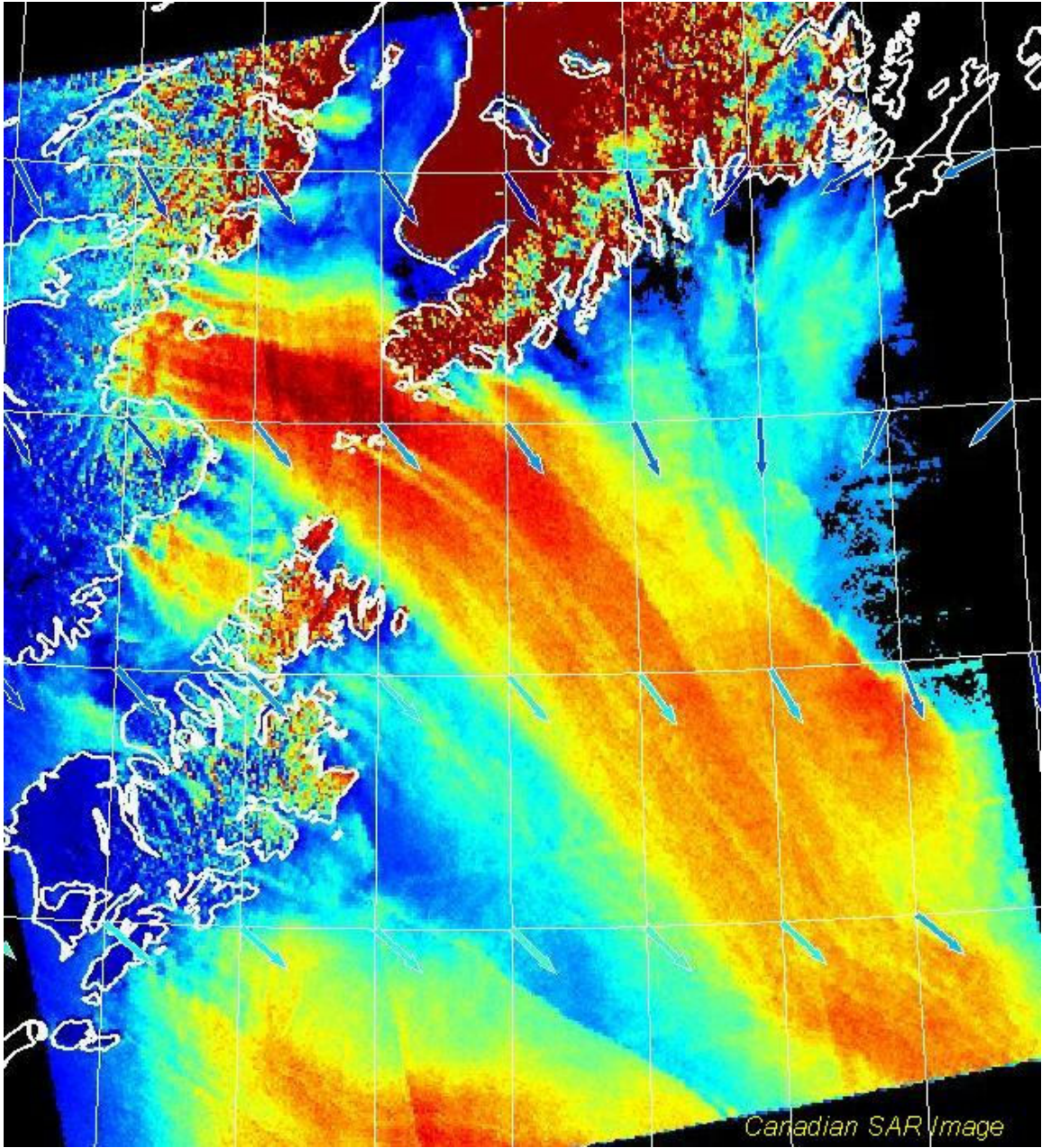


Figure 4.

A strong synoptic northwest wind event at 0004 UTC, 13 October, 1999. Wind speed scale as in Figure 2.

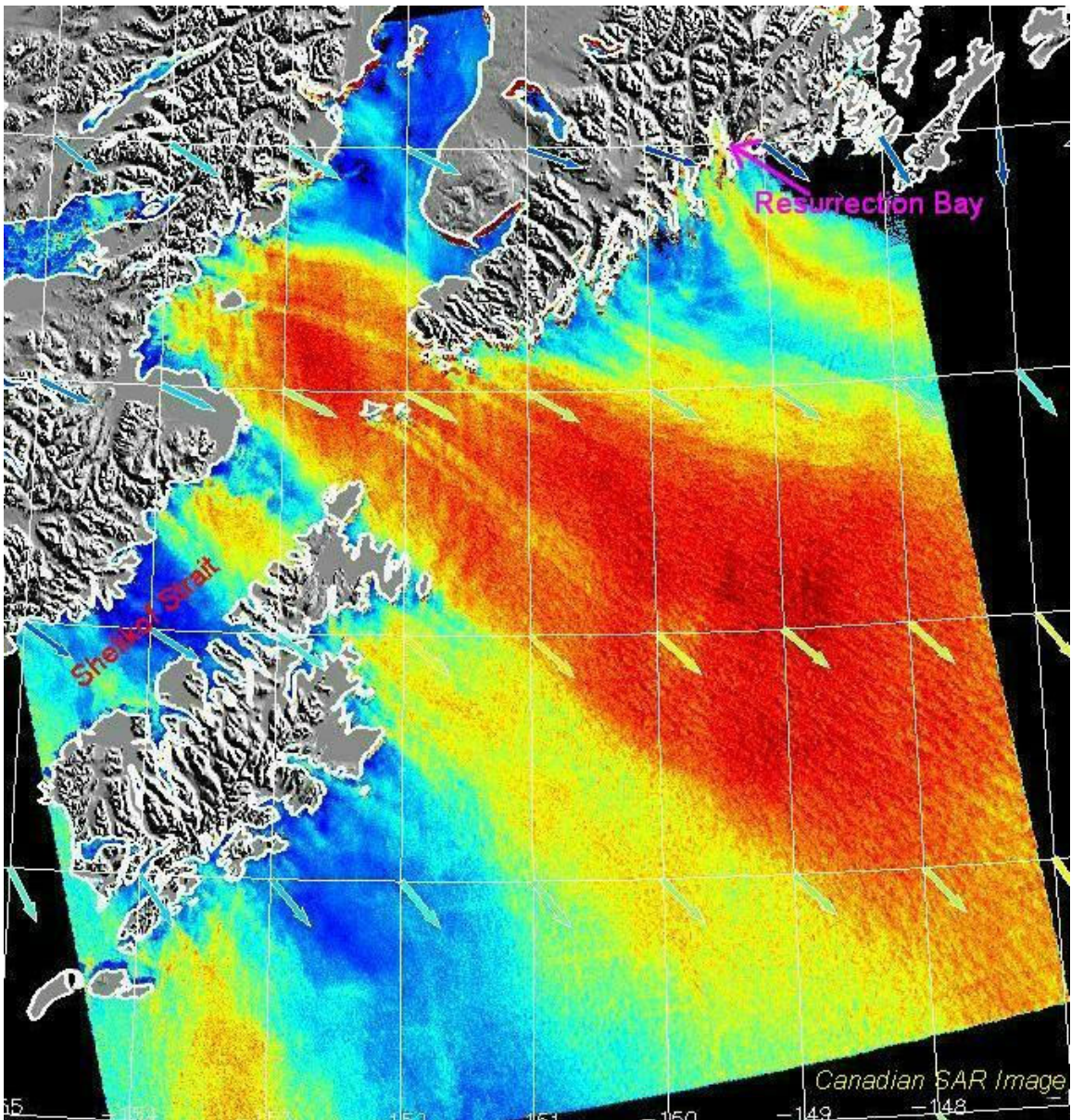


Figure 5.

A strong synoptic northwest event at 0004 UTC, 24 December, 1999. Wind speed scale as in Figure 2.

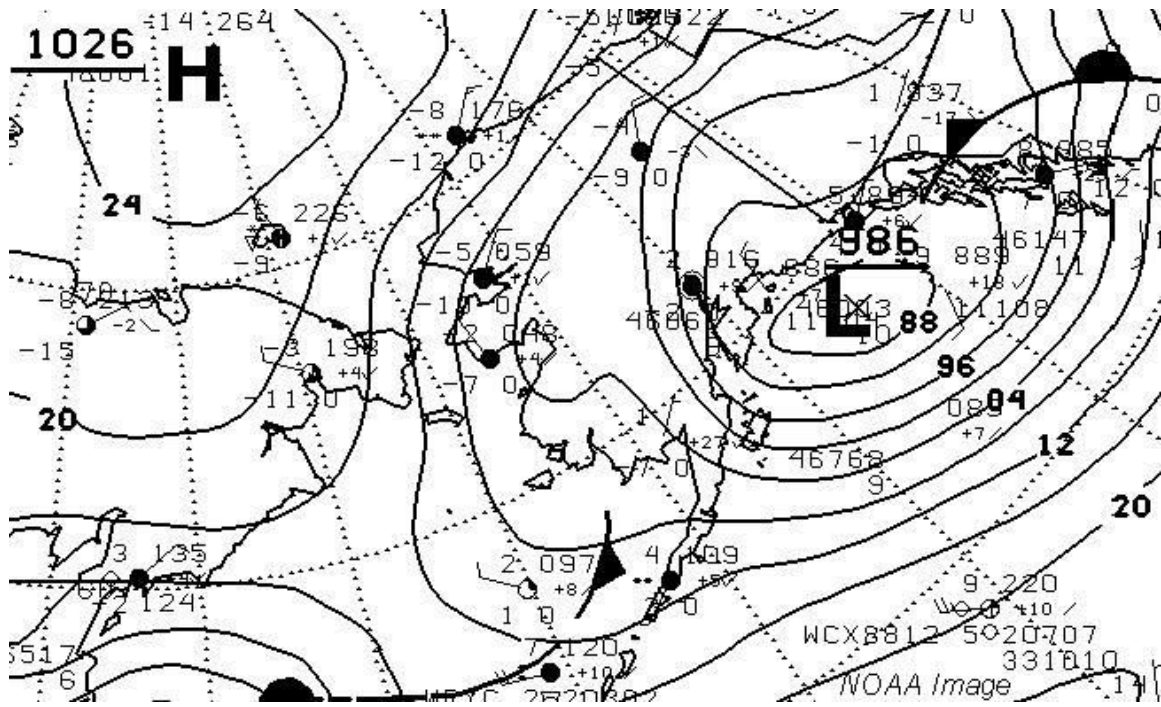


Figure 6.

Corresponding NCEP surface pressure analysis at 0006 UTC, 13 October, 1999 to wind event in Figure 4.

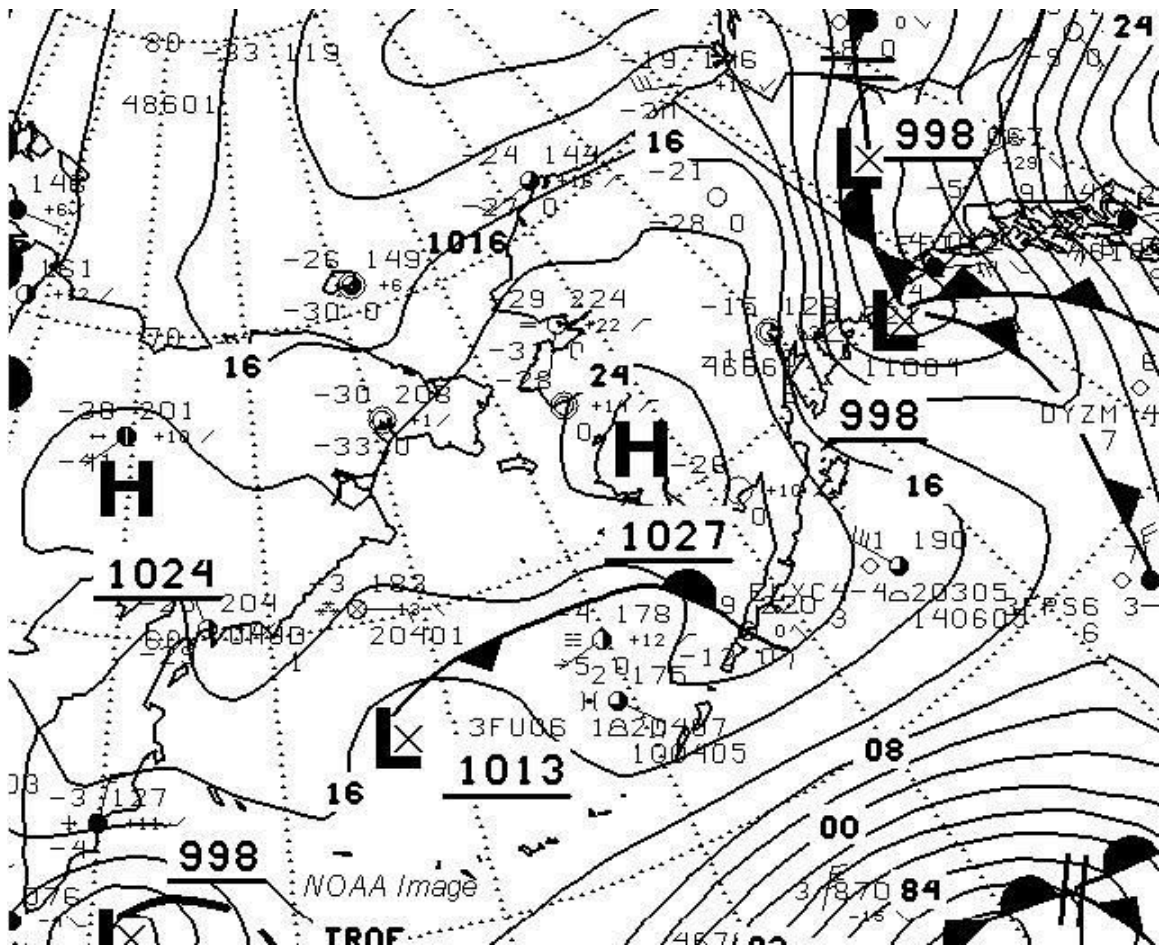


Figure 7.

Corresponding NCEP surface pressure analysis at 0006 UTC, 24 December, 1999 to wind event displayed in Figure 5.

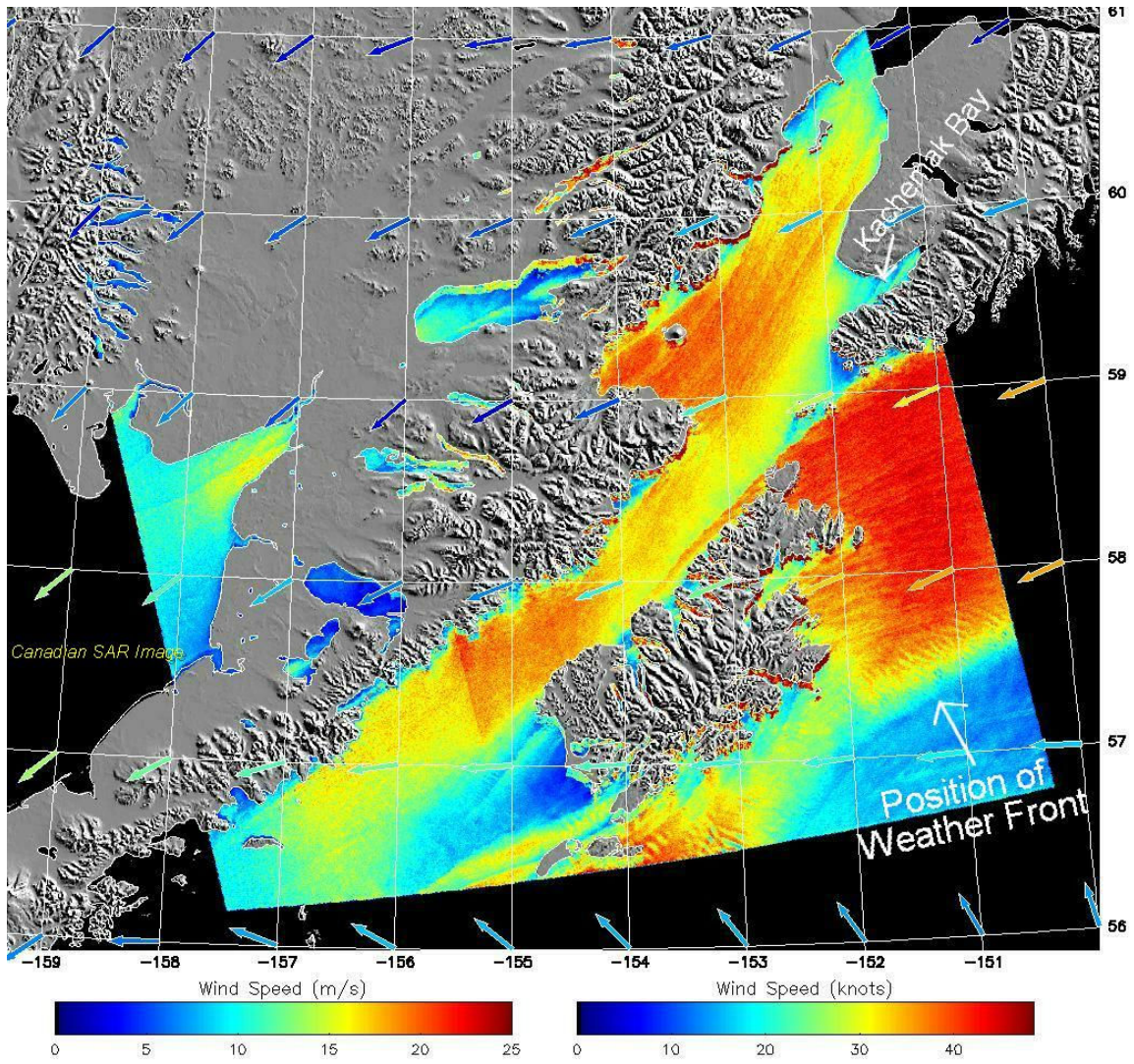


Figure 8.

A strong synoptic northeast wind event at 0004 UTC, 16 October, 1999. Wind speed scale as in Figure 2.



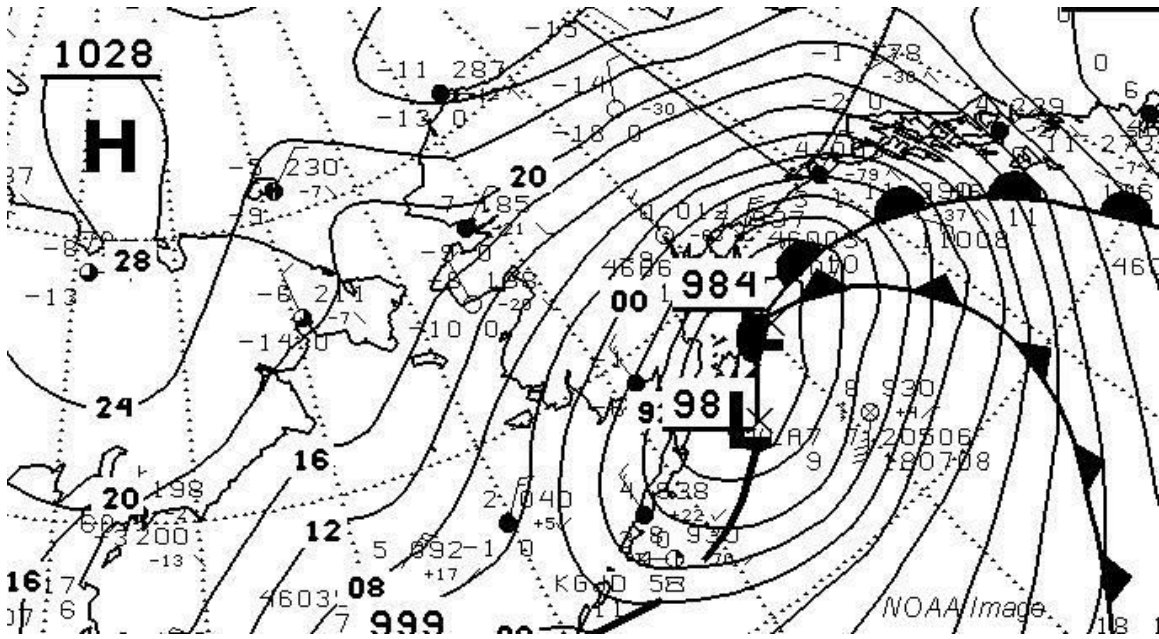


Figure 9.

Corresponding NCEP surface pressure analysis at 0006 UTC, 16 October, 1999. Wind scale as in Figure 2.

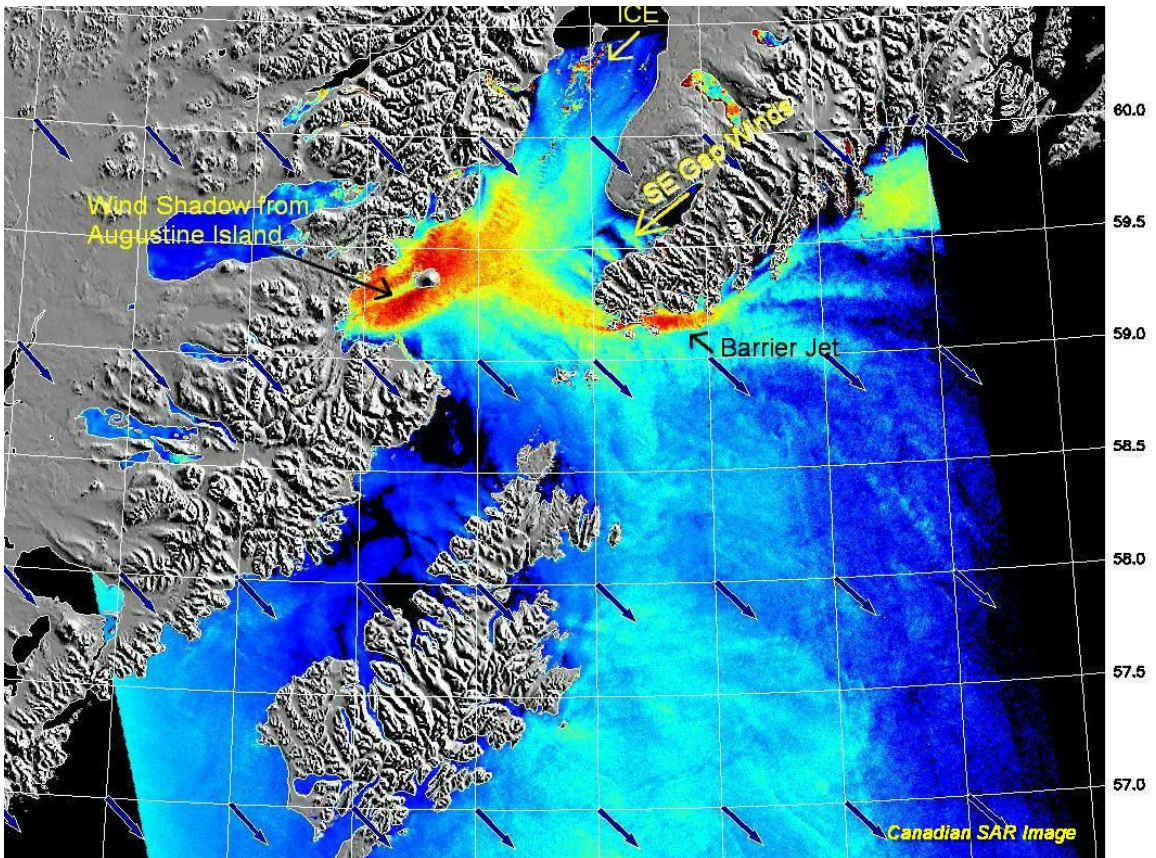


Figure 10.

A northeast synoptic wind event at 0006 UTC, 1 March 2004. Wind scale as in Figure 2.